

# Localized versus itinerant states created by multiple oxygen vacancies in SrTiO<sub>3</sub>

Harald O. Jeschke, Juan Shen, and Roser Valentí

*Institut für Theoretische Physik, Goethe-Universität Frankfurt am Main, 60438 Frankfurt am Main, Germany*

(Dated: February 29, 2024)

Oxygen vacancies in strontium titanate surfaces (SrTiO<sub>3</sub>) have been linked to the presence of a two-dimensional electron gas with unique behavior. We perform a detailed density functional theory study of the lattice and electronic structure of SrTiO<sub>3</sub> slabs with multiple oxygen vacancies, with a main focus on two vacancies near a titanium dioxide terminated SrTiO<sub>3</sub> surface. We conclude based on total energies that the two vacancies preferably inhabit the first two layers, *i.e.* they cluster vertically, while in the direction parallel to the surface, the vacancies show a weak tendency towards equal spacing. Analysis of the nonmagnetic electronic structure indicates that oxygen defects in the surface TiO<sub>2</sub> layer lead to population of Ti  $t_{2g}$  states and thus itinerancy of the electrons donated by the oxygen vacancy. In contrast, electrons from subsurface oxygen vacancies populate Ti  $e_g$  states and remain localized on the two Ti ions neighboring the vacancy. We find that both, the formation of a bound oxygen-vacancy state composed of hybridized Ti  $3e_g$  and  $4p$  states neighboring the oxygen vacancy as well as the elastic deformation after extracting oxygen contribute to the stabilization of the in-gap state.

PACS numbers: 71.55.-i, 73.20.-r, 71.15.Mb, 74.20.Pq

**Introduction.** The discovery of a two-dimensional electron gas at the interface between SrTiO<sub>3</sub> (STO) and LaAlO<sub>3</sub> (LAO) in an LAO/STO heterostructure by Ohtomo and Hwang [1] initiated intense research efforts [2, 3] on these materials and unexpected phases at the interface like superconductivity [4] and ferromagnetism [5] were reported. However, there has been some controversy on the mechanisms leading to the conducting interface, with proposals ranging from electronic reconstruction as a way to avoid a polar catastrophe [6] to various mechanisms based on extrinsic defects like oxygen vacancies [7, 8] and site disorder [9, 10]. More recently, a metallic state has also been discovered at the surfaces of freshly cleaved SrTiO<sub>3</sub> [11, 12] and KTaO<sub>3</sub> [13]. In the case of pure SrTiO<sub>3</sub> surfaces, the metallic state and the photoemission spectra can be well explained with oxygen vacancies [11, 14, 15]. Besides the spectral weight at the Fermi level, the presence of a peak at about 1.3 eV below the Fermi level was also reported [11]. Aiura *et al.* [16] observed in photoemission experiments for lightly electron-doped SrTiO<sub>3</sub> under different oxygen pressure conditions, that the peak at 1.3 eV appears to depend on the oxygen defect density. As pristine SrTiO<sub>3</sub> is a semiconductor with a large band gap of  $E_g = 3.2$  eV. Therefore, creating a number of Ti  $t_{2g}$  carriers and assuming a rigid band shift should lead to a photoemission spectrum with a wide gap below the states near the Fermi level. However, several experiments [11, 12, 16–19] show that the  $E = -1.3$  eV feature is robust and reproducible but sensitive to oxygen pressure. Understanding the nature and orbital character of the  $E = -1.3$  eV feature as well as the interplay between localized and itinerant states created by the presence of oxygen vacancies will be the main focus of our study. In fact, the role of oxygen vacancies is presently being intensively discussed in a wider context of materials. For instance, oxygen vacancies have been proposed to be responsible for the suppression of the metal-insulator transition in VO<sub>2</sub> [20], as well as for the electron beam-induced growth of iron nanowires on TiO<sub>2</sub> [21], to mention a few. Therefore, getting a deeper microscopic understanding of the role of oxy-

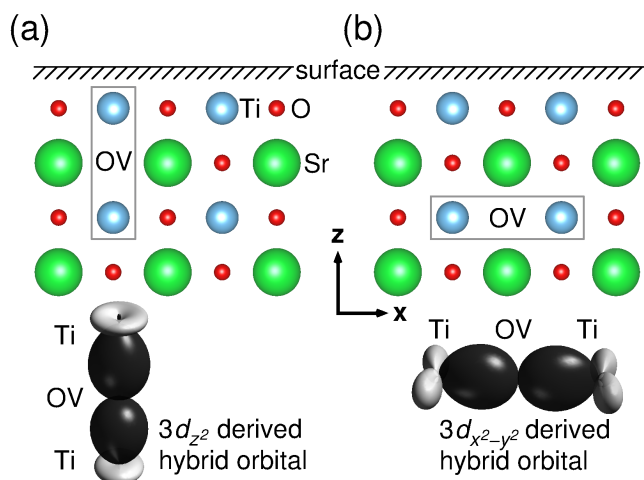


FIG. 1: (Color online) Schematic view of two inequivalent subsurface oxygen vacancy positions together with a sketch of the symmetry of the resulting hybrid orbitals on the Ti sites next to the oxygen vacancy.

gen vacancies in transition metal oxides can further elucidate the mechanisms behind the above observed phenomena.

There have been a number of previous theoretical efforts dealing with oxygen vacancies in SrTiO<sub>3</sub>. Hou and Terakura [22] performed GGA+U calculations of single and double oxygen vacancies in bulk SrTiO<sub>3</sub>. Several calculations based on hybrid functionals [23, 24] or LDA+U [25] find an oxygen defect related in-gap state for SrTiO<sub>3</sub>. Lin and Demkov [26] use a three-orbital Hubbard orbital to study the effect of electronic correlation on an oxygen vacancy in SrTiO<sub>3</sub>. Pavlenko *et al.* [27] have analyzed the orbital reconstruction at SrTiO<sub>3</sub>/LaAlO<sub>3</sub> interfaces due to oxygen vacancies within GGA+U. We will extend this existing work by (i) focusing on SrTiO<sub>3</sub> surfaces and by (ii) using large supercells that allow us to investigate two and three oxygen vacancies at realistic defect densities.

In our study we show that (i) multiple subsurface oxygen defects are energetically less favorable than configurations with at least one defect in the  $\text{TiO}_2$  surface layer. (ii) Vertically, defects show a clear tendency to cluster; defect configurations with two oxygen defects in the first two layers (surface  $\text{TiO}_2$  and first subsurface SrO layer) are clearly preferred over configurations with one or two layers of vertical distance between the two vacancies. In contrast, in the direction parallel to the surface, we find a tendency of vacancies to distribute uniformly. (iii) Moreover, while the isolated surface oxygen vacancy creates itinerant  $\text{Ti } t_{2g}$  electrons, the subsurface vacancy creates two localized states of  $\text{Ti } e_g$  character in the two adjacent Ti ions. The localized states have  $3d_{z^2}$  character with some  $4p_z$  weight for oxygen vacancies in a subsurface SrO layer, and  $3d_{x^2-y^2}$  character with some  $4p_x/p_y$  weight for vacancies in a subsurface  $\text{TiO}_2$  layer (see Fig. 1). Finally, we also show that (iv) the precise condition for an in-gap state produced from surface vacancies is the formation of a  $\text{TiO}_3(\text{vacancy})_2$  cluster.

**Method.** In order to investigate the role of oxygen vacancies in  $\text{SrTiO}_3$ , we performed density functional theory calculations for a number of  $\text{SrTiO}_3$  slabs with various configurations of oxygen vacancies and analyzed the origin of the states appearing near the Fermi level. We have considered stoichiometric  $\text{SrTiO}_3$  slabs with (001) surfaces, as discussed in Ref. 14. Based on our previous experience, we focus on  $3 \times 3 \times 4$  supercells with (a)  $\text{TiO}_2$  and (b) SrO termination. We use the energetically most favorable structures with a single vacancy in the  $\text{TiO}_2$  or SrO surface layer as starting point for structures with a second or even a third oxygen defect. We relax these structure candidates using the Vienna *ab initio* simulation package (VASP) [28, 29] with the projector augmented wave (PAW) basis [30]. As it has been found that relaxations with the generalized gradient approximation (GGA) tend to make the octahedral environment of transition metal ions too homogeneous [31] we use a GGA+U functional [32] with literature values for  $\text{SrTiO}_3$  [33] of  $U = 5$  eV and  $J = 0.64$  eV. We analyze the electronic structure and total energy of the predicted slab geometries using an all electron full potential local orbital (FPLO) [34] basis.

**Results.** In Figure 2, we show examples of  $\text{SrTiO}_3$  supercells with two oxygen vacancies. They correspond to the energetically most favorable configurations with the first vacancy in the  $\text{TiO}_2$  surface layer (layer 1) and the second vacancy in (a) the surface layer (layer 1), (b) the first subsurface SrO layer (layer 2), (c) the first subsurface  $\text{TiO}_2$  layer (layer 3) or (d) the second subsurface SrO layer (layer 4). An overview of the energetics is shown in Figure 3. Energies are given with respect to the energy  $E_0$  of the configuration drawn in Figure 2 (b) which turned out to be the optimum. We find a clear trend: Defect configurations with one vacancy on the surface (layer 1) and the second one in the first subsurface layer (layer 2) are energetically more favorable than configurations where the two oxygen vacancies are separated by one or two pristine layers. This means that there is a clear tendency of oxygen vacancies to cluster vertically near the surface of  $\text{SrTiO}_3$ . In the direction parallel to the surface, however, the outcome of our simulations is more complex. While configurations with both

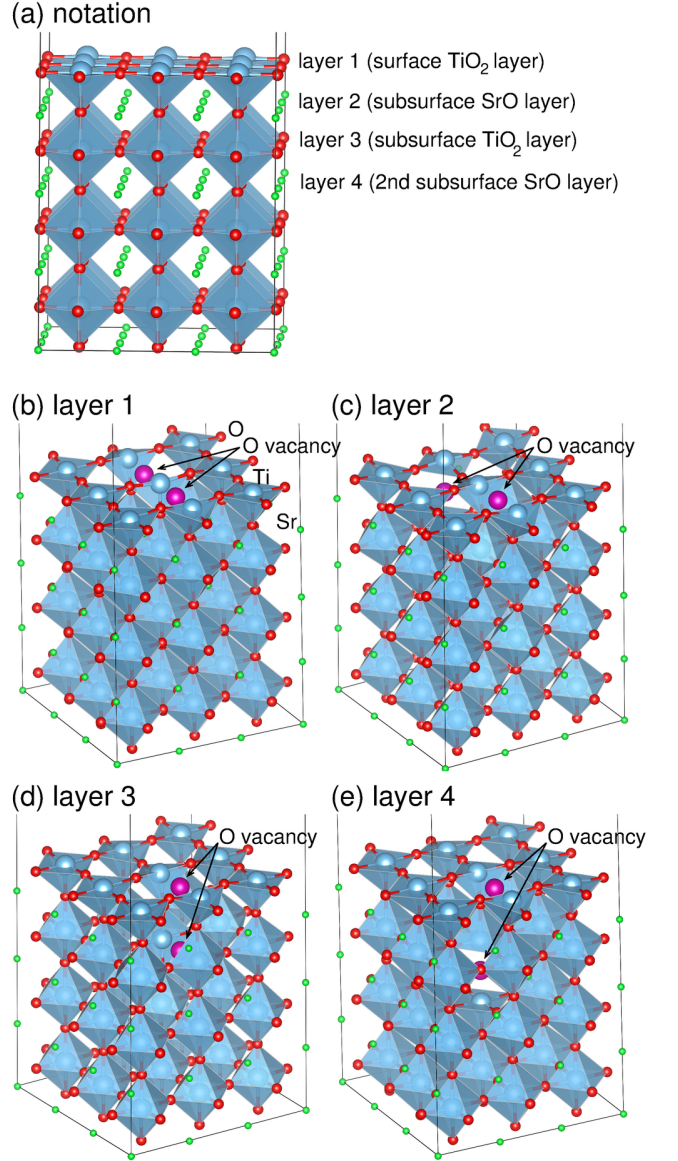


FIG. 2: (Color online) Examples of  $\text{SrTiO}_3$  slab structures.  $3 \times 3 \times 4$  perovskite units have been considered in the calculation and in (a) the notation used through the text is given. There are two oxygen vacancies: one is always in the surface  $\text{TiO}_2$  layer (layer 1). Examples for the energetically most favorable positioning of the second oxygen vacancy in the surface layer (layer 1) is shown in (b), in the subsurface SrO layer (layer 2) in (c), in the first subsurface  $\text{TiO}_2$  layer (layer 3) in (d) and in the second subsurface SrO layer (layer 4) in (e).

defects in the surface  $\text{TiO}_2$  layer (circles in Figure 3) show a weak tendency to cluster, the energetically most favorable corresponds to distributing one defect in the first ( $\text{TiO}_2$ ) and one defect in the second (SrO) layer (triangle at  $E = E_0$  in Figure 3) with a maximal distance between the two vacancies within our simulation cell. This result suggests a tendency to uniform distribution of defects parallel to the surface. Turning to the defects separated by a pristine SrO layer from the surface oxygen defect (diamonds in Figure 3), we observe a weak preference of defects to lower vacancy-vacancy separa-

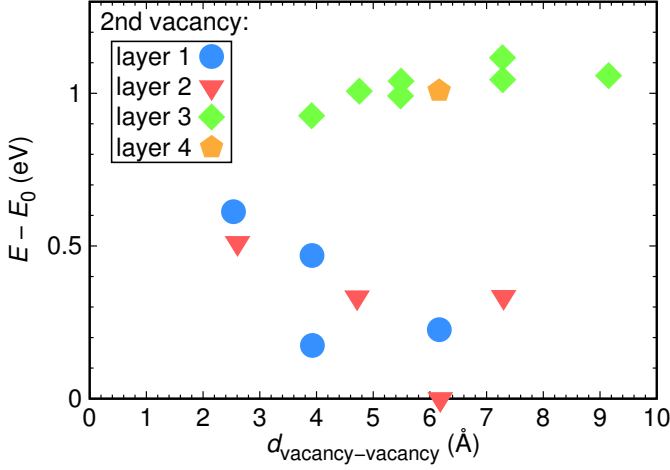


FIG. 3: (Color online) Total energies of SrTiO<sub>3</sub> slabs with two oxygen vacancies calculated within GGA+U. The first vacancy is always in the surface TiO<sub>2</sub> layer (layer 1). Energies are given as function of distance to the second vacancy which can be in the surface TiO<sub>2</sub> layer (layer 1) (circles), in the subsurface SrO layer (layer 2) (triangles), in the first subsurface TiO<sub>2</sub> layer (layer 3) (diamonds) or in the second subsurface SrO layer (layer 4) (pentagon).

tion, *i. e.* to cluster with the SrO spacer layer between the two defects.

We now proceed with an analysis of the electronic structure of the two oxygen vacancy configurations. Figure 4 shows the density of states for all structures discussed before. Gray shading indicates electronic states which are populated with electrons donated by the oxygen vacancy. All investigated structures have Ti  $t_{2g}$  weight near the Fermi level. A detailed analysis of this weight shows that a large amount of Ti ions in the supercell contribute to it and the corresponding bands are dispersive, indicating that these electrons are itinerant. We have shown in Ref. 14 that this is a result of structural relaxation; if all ions are kept in the ideal perovskite position upon creation of an oxygen vacancy, only Ti  $t_{2g}$  orbitals next to the vacancy are occupied, and an unphysical localized  $t_{2g}$  electron density is created. As a second important feature, all structures in Figure 4 (b) and all except the first one in Figure 4 (a) also show sharp in-gap states; these are states typically created by subsurface oxygen defects and localized on the two Ti ions adjacent to the defect. These states have Ti  $e_g$  character with small admixture of  $4p$  states, and they clearly fall into two categories: Ti  $d_{z^2}$  states created by vacancies in a SrO layer, and Ti  $d_{x^2-y^2}$  states produced by vacancies in subsurface TiO<sub>2</sub> layers. This orbital occupancy is due to the fact that in the case of an oxygen defect in a SrO layer, the Ti ions neighboring the defect are above and below the defect where the vertical axis corresponds to the  $z$  axis in the orbital projection (see Fig. 1 (a)). In the case of a subsurface defect in a TiO<sub>2</sub> layer, the two neighboring Ti ions sit at half a lattice spacing either along  $x$  or along  $y$  direction with respect to the vacancy (see Fig. 1 (b)). Figure 5 (a) illustrates the orbital distribution of the defect configuration shown in Figure 2 (b) where one vacancy is on the TiO<sub>2</sub> surface (layer 1) and the second vacancy is on the

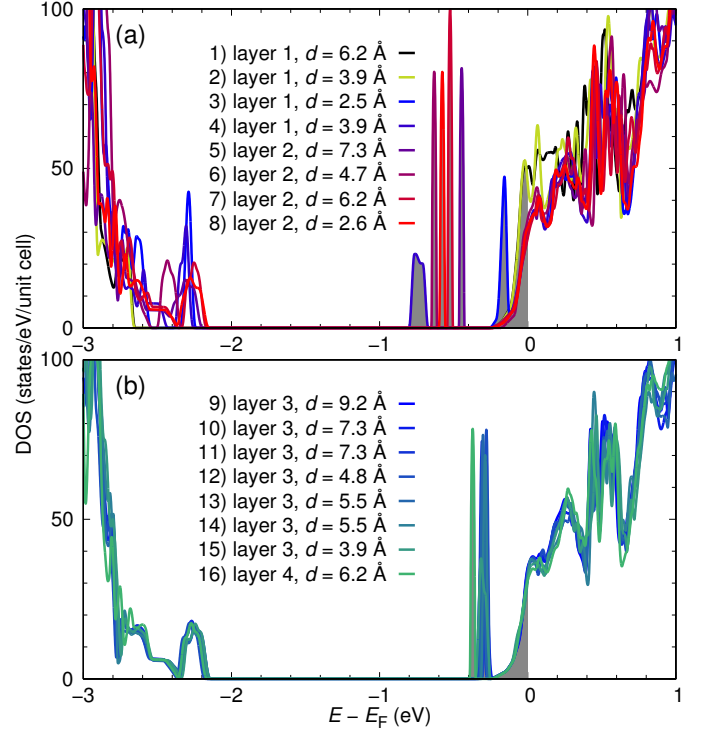


FIG. 4: (Color online) Densities of states for two oxygen vacancies in  $3 \times 3 \times 4$  SrTiO<sub>3</sub> slabs calculated within GGA+U. The first vacancy is always in the surface TiO<sub>2</sub> layer. (a) Second vacancy in surface TiO<sub>2</sub> layer or in first subsurface SrO layer. All but the first two structures lead to an in-gap DOS peak. In the structure corresponding to DOS number 4, the two oxygen vacancies have a Ti in the middle, in contrast to DOS number 2. (b) Second vacancy in first surface TiO<sub>2</sub> layer or in second subsurface SrO layer. Number 4 is the DOS for the structure in Fig. 2 (a), number 8 corresponds to Fig. 2 (b), number 15 to Fig. 2 (c) and number 16 to Fig. 2 (d).

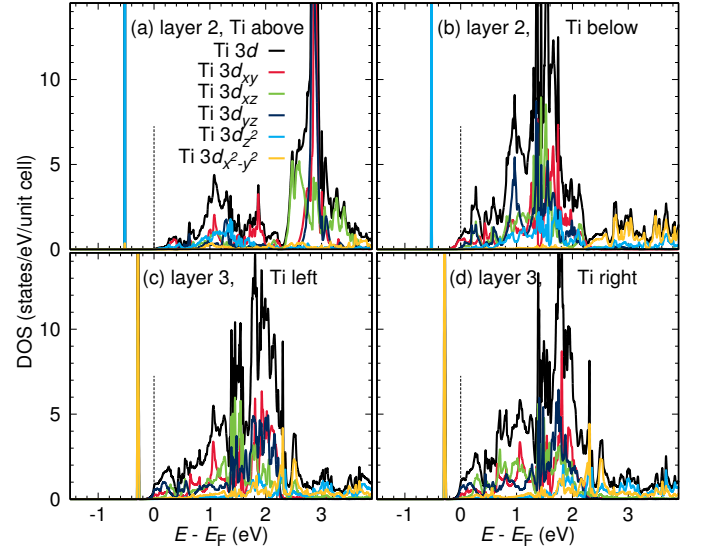


FIG. 5: (Color online) Partial densities of states for Ti ions neighboring oxygen vacancies. (a) and (b) Ti ions sitting above and below a vacancy in the first subsurface SrO layer. (c) and (d) Ti ions sitting right and left of a vacancy in the first subsurface TiO<sub>2</sub> layer.



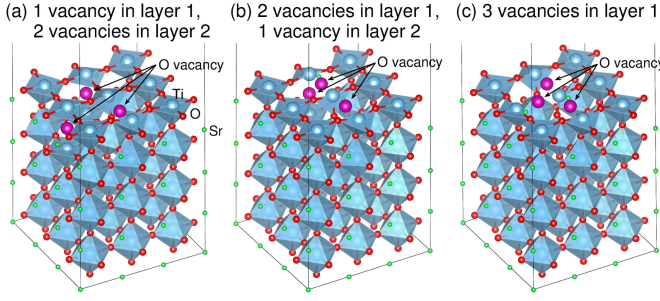


FIG. 6: (Color online) Three examples of three oxygen vacancy configurations in  $3 \times 3 \times 4$  SrTiO<sub>3</sub> slabs.

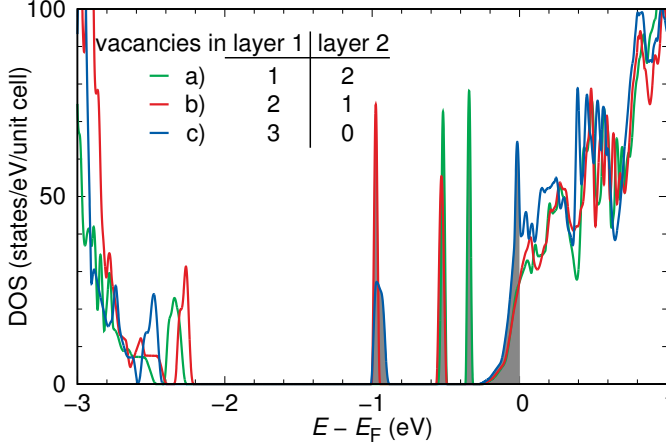


FIG. 7: (Color online) Densities of states for three examples of three oxygen vacancy configurations in  $3 \times 3 \times 4$  SrTiO<sub>3</sub> slabs calculated within GGA+U.

subsurface SrO layer (layer 2). Figure 5 (b) displays the orbital distribution for a representative example of one vacancy on the TiO<sub>2</sub> surface (layer 1) and the second one on the TiO<sub>2</sub> subsurface (layer 3), as in Figure 2 (c).

In-gap states are also present when oxygen vacancies cluster at the surface TiO<sub>2</sub> layer (cases 3 and 4 in Fig. 4). Our calculations show that the precise condition for such in-gap states produced from surface vacancies is the formation of a TiO<sub>3</sub>(vacancy)<sub>2</sub> cluster. In fact, the energetically most favorable configuration with two vacancies in the surface TiO<sub>2</sub> layer (see Figure 2 (a)) is of this type. On the other hand, well separated oxygen vacancies in the surface TiO<sub>2</sub> layer which form TiO<sub>4</sub>(vacancy) clusters only (cases 1 and 2 in Fig. 4) lead to an itinerant 2D electron gas of Ti  $t_{2g}$  electrons but no in-gap states.

In order to further test the distribution of oxygen-vacancy-induced extra charge, we also calculated the electronic properties of  $3 \times 3 \times 4$  SrTiO<sub>3</sub> slabs with three oxygen vacancy configurations as shown in Fig. 6. In all three cases in-gap states appear below the Fermi level since some oxygen vacancies are either below the TiO<sub>2</sub> surface layer or they are clustered around a Ti on the surface. Comparison of the two-vacancy with the three-vacancy cases shows that the in-gap weight is

proportional to the oxygen vacancy density. This observation is in qualitative agreement with experiment [16] but it should be investigated further.

**Discussion.** Analysis of the previous LDA+U results allows us to draw some important conclusions regarding the role of oxygen vacancies in SrTiO<sub>3</sub>. (1) If oxygen vacancies are only on the surface and well separated from each other, the two electrons per vacancy contribute *only* to the conduction band and no localized in-gap states are formed independently of the  $U$  value considered in the LDA+U calculations. Only when oxygen vacancies cluster on the surface, assuming TiO<sub>3</sub>(vacancy)<sub>2</sub> configurations, or are positioned in subsurface layers do we observe the formation of in-gap states coming from the hybridized  $3e_g$  with  $4p$  states from the Ti neighboring the vacancy. This is in contrast to a recent study by Lin *et al.* [26] where it was suggested that the oxygen-vacancy induced in-gap state traps at most one electron from the oxygen vacancy while the second electron contributes to the conduction. (2) The energy ordering of the different vacancies configurations with presence of in-gap states can be attributed to two effects: (i) the gain in energy due to the formation of a bound oxygen-vacancy state (in-gap state) composed of the hybridized Ti  $e_g$  and  $4p$  states neighboring the vacancy as well as (ii) the gain in elastic energy due to the lattice deformation after extracting oxygen. In fact, calculations of total energies of relaxed versus unrelaxed slab structures point to a significant contribution of the second effect that should be considered together with the formation of the bound state. Moreover, the lattice deformation is important in the formation of an itinerant 2D electron gas due to surface oxygen vacancies. (3) The weight of the in-gap state scales with the oxygen vacancy concentration in agreement with photoemission experiments. (4) The formation energy of an oxygen vacancy in SrTiO<sub>3</sub> is about 7.7 eV for a single vacancy and 4.8 eV per vacancy for two and three vacancies. From our present calculations we can only speculate about possible formation mechanisms of such vacancies. Certainly the exposure to energetic photons in photoemission experiments is a possible cause.

In summary, by considering different configurations of oxygen vacancies in SrTiO<sub>3</sub> and subsequent analysis of the energetics and electronic properties via extensive DFT calculations we can explain the origin of observed in-gap states as well as conduction electrons in photoemission experiments on SrTiO<sub>3</sub> surfaces and provide predictions for the behavior of a finite concentration of oxygen vacancies in SrTiO<sub>3</sub>.

### Acknowledgments

We thank Ralph Claessen, Michael Sing, Andres Santander-Syro, Marc Gabay and Marcelo Rozenberg for useful discussions and gratefully acknowledge financial support by the Deutsche Forschungsgemeinschaft (DFG) through grant FOR 1346. The generous allotment of computer time by CSC-Frankfurt and LOEWE-CSC is also gratefully acknowledged.

- [1] A. Ohtomo and H. Y. Hwang, *A high-mobility electron gas at the  $\text{LaAlO}_3/\text{SrTiO}_3$  heterointerface*, Nature (London) **427**, 423 (2004).
- [2] J. Mannhart, D. H. A. Blank, H. Y. Hwang, A. J. Millis and J.-M. Triscone, *Two-dimensional electron gases at oxide interfaces*, MRS Bulletin **33**, 1027 (2008).
- [3] M. Huijben, A. Brinkman, G. Koster, G. Rijnders, H. Hilgenkamp, and D. H. A. Blank, *Structure-Property Relation of  $\text{SrTiO}_3/\text{LaAlO}_3$  Interfaces*, Adv. Mater. **21**, 1665 (2009).
- [4] N. Reyren, S. Thiel, A. Caviglia, L. Fitting-Kourkoutis, G. Hammerl, C. Richter, C.W. Schneider, T. Kopp, A.-S. Rüetschi, D. Jaccard, M. Gabay, D. A. Muller, J.-M. Triscone, J. Mannhart, *Superconducting Interfaces Between Insulating Oxides*, Science **317**, 1196 (2007).
- [5] A. Brinkmann, M. Huijben, M. van Zalk, J. Huijben, U. Zeitler, J.C. Maan, W. G. van der Wiel, G. Rijnders, D. H. A. Blank, H. Hilgenkamp, *Magnetic effects at the interface between non-magnetic oxides*, Nat. Mater. **6**, 493 (2007).
- [6] S. Okamoto, A. J. Millis, *Electronic reconstruction at an interface between a Mott insulator and a band insulator*, Nature **428**, 630 (2004).
- [7] W. Siemons, G. Koster, H. Yamamoto, W. A. Harrison, G. Lucovsky, T. H. Geballe, D. H. A. Blank, and M. R. Beasley, *Origin of charge density at  $\text{LaAlO}_3$  on  $\text{SrTiO}_3$  heterointerfaces: Possibility of intrinsic doping*, Phys. Rev. Lett. **98**, 196802 (2007).
- [8] G. Herranz, M. Basletić, M. Bibes, C. Carrétéro, E. Tafrá, E. Jacquet, K. Bouzehouane, C. Deranlot, A. Hamzić, J.-M. Broto, A. Barthélémy, and A. Fert, *High mobility in  $\text{LaAlO}_3/\text{SrTiO}_3$  heterostructures: Origin, dimensionality, and perspectives*, Phys. Rev. Lett. **98**, 216803 (2007).
- [9] N. Nakagawa, H. Y. Hwang, and D. A. Muller, *Why some interfaces cannot be sharp*, Nat. Mater. **5**, 204 (2006).
- [10] L. Li and A. Zunger, *A unifying mechanism for conductivity and magnetism at interfaces of insulating nonmagnetic oxides*, arXiv:1402.0895 (unpublished).
- [11] A. F. Santander-Syro, O. Copie, T. Kondo, F. Fortuna, S. Pailhès, R. Weht, X. G. Qiu, F. Bertran, A. Nicolaou, A. Taleb-Ibrahimi, P. Le Fèvre, G. Herranz, M. Bibes, N. Reyren, Y. Apertet, P. Lecoeur, A. Barthélémy, and M. J. Rozenberg, *Two-dimensional electron gas with universal subbands at the surface of  $\text{SrTiO}_3$* , Nature (London) **469**, 189 (2011).
- [12] W. Meevasana, P. D. C. King, R. H. He, S.-K. Mo, M. Hashimoto, A. Tamai, P. Songsiririthigul, F. Baumberger, and Z.-X. Shen, *Creation and control of a two-dimensional electron liquid at the bare  $\text{SrTiO}_3$  surface*, Nat. Mater. **10**, 114 (2011).
- [13] P. D. C. King, R. H. He, T. Eknapakul, P. Buaphet, S.-K. Mo, Y. Kaneko, S. Harashima, Y. Hikita, M. S. Bahramy, C. Bell, Z. Hussain, Y. Tokura, Z.-X. Shen, H.Y. Hwang, F. Baumberger, and W. Meevasana, *Subband Structure of a Two-Dimensional Electron Gas Formed at the Polar Surface of the Strong Spin-Orbit Perovskite  $\text{KTaO}_3$* , Phys. Rev. Lett. **108**, 117602 (2012).
- [14] J. Shen, H. Lee, R. Valentí, and H. O. Jeschke, *Ab initio study of the two-dimensional metallic state at the surface of  $\text{SrTiO}_3$ : Importance of oxygen vacancies*, Phys. Rev. B **86**, 195119 (2012).
- [15] Z. Wang, Z. Zhong, X. Hao, S. Gerhold, B. Stöger, M. Schmid, J. Sanchez-Barriga, A. Varykhalov, C. Franchini, K. Held, U. Diebold, *Anisotropic two-dimensional electron gas at  $\text{SrTiO}_3(110)$* , Proc. Natl. Acad. Sci. USA **111**, 3933 (2014).
- [16] Y. Aiura, I. Hase, H. Bando, T. Yasue, T. Saitoh, and D. S. Dessau, *Photoemission study of the metallic state of lightly electron-doped  $\text{SrTiO}_3$* , Surf. Sci. **515**, 61 (2002).
- [17] R. Courths, *Ultraviolet photoelectron spectroscopy (UPS) and LEED studies of  $\text{BaTiO}_3(001)$  and  $\text{SrTiO}_3(100)$  surfaces*, Phys. Stat. Sol. B **100**, 135 (1980).
- [18] Y. S. Kim, J. Kim, S. J. Moon, W. S. Choi, Y. J. Chang, J.-G. Yoon, J. Yu, J.-S. Chung, and T. W. Noh, *Localized electronic states induced by defects and possible origin of ferroelectricity in strontium titanate thin films*, Appl. Phys. Lett. **94**, 202906 (2009).
- [19] R. C. Hatch, K. D. Fredrickson, M. Choi, C. Lin, H. Seo, A. B. Posadas, and A. A. Demkov, *Surface electronic structure for various surface preparations of Nb-doped  $\text{SrTiO}_3(001)$* , J. Appl. Phys. **114**, 103710 (2013).
- [20] J. Jeong, N. Aetukuri, T. Graf, T. D. Schladt, M. G. Samant, S. T. P. Parkin, *Suppression of metal-insulator transition in  $\text{VO}_2$  by electric field-induced oxygen vacancy formation* Science, **339**, 1402 (2013).
- [21] F. Vollnhals, T. Woolcot, M.-M. Walz, S. Seiler, H.-P. Steinrück, G. Thornton, H. Marbach, *Electron Beam-Induced Writing of Nanoscale Iron Wires on a Functional Metal Oxide* Journal of Physical Chemistry C **117**, 17674 (2013).
- [22] Z. Hou and K. Terakura, *Defect States Induced by Oxygen Vacancies in Cubic  $\text{SrTiO}_3$ : First-Principles Calculations*, J. Phys. Soc. Jpn. **79**, 114704 (2010).
- [23] C. Mitra, C. Lin, J. Robertson, and A. A. Demkov, *Electronic structure of oxygen vacancies in  $\text{SrTiO}_3$  and  $\text{LaAlO}_3$* , Phys. Rev. B **86**, 155105 (2012).
- [24] J. Carrasco, F. Illas, N. Lopez, E. A. Kotomin, Yu. F. Zhukovskii, R. A. Evarestov, Yu. A. Mastrikov, S. Piskunov, and J. Maier, *First-principles calculations of the atomic and electronic structure of F centers in the bulk and on the  $(001)$  surface of  $\text{SrTiO}_3$* , Phys. Rev. B **73**, 064106 (2006).
- [25] C. Lin, C. Mitra, and A. A. Demkov, *First-principles calculations of the atomic and electronic structure of F centers in the bulk and on the  $(001)$  surface of  $\text{SrTiO}_3$* , Phys. Rev. B **86**, 161102(R) (2012).
- [26] C. Lin and A. A. Demkov, *Electron correlation in oxygen vacancy in  $\text{SrTiO}_3$* , Phys. Rev. Lett. **111**, 217601 (2013).
- [27] N. Pavlenko, T. Kopp, E. Y. Tsybmal, J. Mannhart, G. A. Sawatzky, *Oxygen vacancies at titanate interfaces: Two-dimensional magnetism and orbital reconstruction*, Phys. Rev. B **86**, 064431 (2012).
- [28] G. Kresse, J. Hafner, *Ab initio molecular dynamics for liquid metals*, Phys. Rev. B **47**, 558 (1993).
- [29] G. Kresse and J. Furthmüller, *Efficiency of ab-initio total energy calculations for metals and semiconductors using a plane-wave basis set*, Comput. Mater. Sci. **6**, 15 (1996).
- [30] P. E. Blöchl, *Projector augmented wave method*, Phys. Rev. B **50**, 17953 (1994).
- [31] K. Foyevtsova, I. Opahle, Y.-Z. Zhang, H. O. Jeschke, R. Valentí, *Determination of effective microscopic models for the frustrated antiferromagnets  $\text{Cs}_2\text{CuCl}_4$  and  $\text{Cs}_2\text{CuBr}_4$  by density functional methods*, Phys. Rev. B **83**, 125126 (2011).
- [32] A. I. Liechtenstein, V. I. Anisimov, and J. Zaanen, *Density functional theory and strong interactions: Orbital ordering in Mott-Hubbard insulators*, Phys. Rev. B **52**, R5467 (1995).
- [33] S. Okamoto, A. J. Millis, N. A. Spaldin, *Lattice Relaxation in Oxide Heterostructures:  $\text{LaTiO}_3/\text{SrTiO}_3$  Superlattices*, Phys. Rev. Lett. **97**, 056802 (2006).
- [34] K. Koepnick and H. Eschrig, *Full-potential nonorthogonal local-orbital minimum-basis band-structure scheme*, Phys. Rev.

B **59**, 1743 (1999); <http://www.FPLO.de>

- [35] J. P. Perdew, K. Burke and M. Ernzerhof, *Generalized gradient approximation made simple*, Phys. Rev. Lett. **77**, 3865 (1996).